LOWLAND TECHNOLOGY INTERNATIONAL SI, Vol. 9, No. 2, 29-37, December 2007
International Association of Lowland Technology (IALT), ISSN 1344-9656

MODELLING STRAIN-SOFTENING BEHAVIOUR OF CLAYEY SOILS

J.-C. Chai[1], J. P. Carter[2] and S. Hayashi[3]

ABSTRACT: A method for modelling the strain-softening behaviour of clayey soils under undrained and/or partially drained conditions is proposed and applied to simulate the mechanical behaviour of undisturbed Ariake clay and lime-stabilized Ariake clay samples under undrained conditions. The proposed method is based on the Modified Cam clay (MCC) model. It is assumed that during the softening process, the strain increments can still be calculated by the MCC model, but the effective stress path is enforced to follow the projection of the critical state line (CSL) in a $p' - q$ plot (i.e., $q = M p'$ where p' is mean effective stress, q is deviator stress and M is the slope of the CSL in the $p' - q$ plot). Therefore the method is not completely rigorous in the applied mechanics sense, rather it is a pragmatic approach. The proposed method has been incorporated into a finite element code and its performance was verified by simulating undrained triaxial compression tests. Subsequently, the method has been applied to simulate the mechanical behaviour of both natural and lime-stabilized Ariake clays. Comparing the simulated results with the test data indicates that the method simulated both the shear strain versus deviator stress curve and the effective stress path reasonably well. However, the results also showed that in the case of the lime-stabilized Ariake clay, the adoption of a high initial stiffness under lower confining stress should be considered. It is suggested that the proposed method can be used to analyze geotechnical problems involving strain-softening behaviour with reasonable accuracy.

Keywords: Strain-softening, numerical modelling, clayey soil, finite element analysis, lime-stabilization

INTRODUCTION

Most natural clayey deposits, as well as lime/cement treated clayey soils, exhibit strain-softening behaviour, which can affect, for example, the stability of an embankment and the bearing capacity of a foundation on this kind of ground. Failure of soil under a foundation normally occurs progressively, and in order to simulate the progressive failure phenomenon, strain-softening material behaviour should be considered. Most existing elasto-plastic soil models for clayey soils have a limited capacity to model strain-softening behaviour. For example, the widely used Modified Cam Clay (MCC) model (Roscoe and Burland, 1968) can only simulate softening for a soil element in a heavily over-consolidated state with a relatively high value of the ratio κ/λ, where λ and κ are respectively the slopes of virgin loading and the unloading-reloading lines in e - lnp' space (e is void ratio).

In this paper a relatively simple method for modelling the strain-softening behaviour of clayey soils is presented. The method has been incorporated into a finite element code and its performance was checked by simulating undrained triaxial compression tests. The method has been applied to simulate the strain-softening behaviour of natural and lime-stabilized Ariake clay samples. The simulated results (shear strain versus deviator stress curves, effective stress paths and variation of excess pore water pressure) are compared with test data reported in the literature, and the effectiveness and limitations of the method are discussed.

MODELLING STRAIN-SOFTENING

General Consideration

Potts et al. (1990) simulated the strain-softening behaviour of soil by reducing the strength parameters (cohesion c' and internal friction angle ϕ') with respect to plastic shear strain (ε_s^p), as illustrated in Fig. 1. In the figure the subscripts $_p$ and $_R$ represent peak and residual states. Carter and Liu (2005) proposed an elasto-plastic model called Structured Cam Clay (SCC) to describe the mechanical behaviour of structured clay soils. This model is capable of simulating strain-softening behaviour, particularly when the effective stress path is constrained to move along the projection of the critical state line (CSL) in a $p' - q$ plot (i.e., $q = Mp'$, where q is deviator stress, p' is effective mean stress and M is the

[1] IALT member, Prof., Department of Civil Engineering, Saga University, 1 Honjo, Saga 840-8502, JAPAN
[2] Pro Vice-Chancellor, Faculty of Engineering and Built Environment, The University of Newcastle, NSW 2308, AUSTRALIA
[3] IALT member, Prof., Institute of Lowland Technology, Saga University, 1 Honjo, Saga 840-8502, JAPAN
Note: Discussion on this paper is open until June 2008

slope of the CSL in the p'-q plot). This enforcement of the stress path is based on experimental evidence which

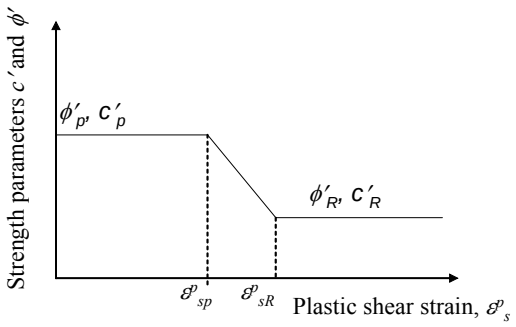

Fig. 1 Empirical strength/shear strain relationship

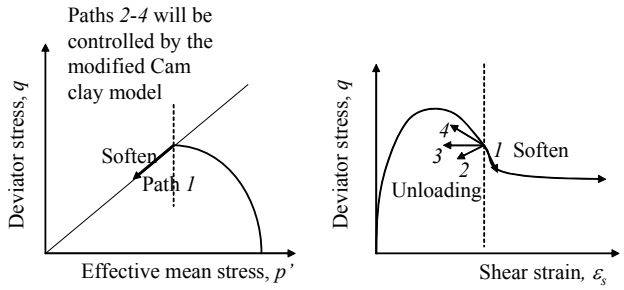

Fig. 2 Possible stress paths after stress state passes the peak

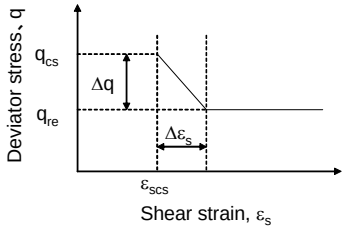

Fig. 3 An empirical shear strain versus deviator stress relationship

indicates that during undrained triaxial tests the effective stress path during softening is often close to the projection of the CSL in p' - q space (it will be simplyreferred as CSL later), i.e., $q = Mp'$ (Adachi et al., 1995; Tanaka, 2000; Tanaka et al., 2001).

The MCC model has been used successfully in describing many important features of the mechanical behaviour of clay. This model only has 5 soil parameters and values for all of them can be determined by conventional laboratory tests, and consequently it has been widely used to simulate the mechanical behaviour of clayey soils in solving geotechnical boundary value problems. For heavily overconsolidated soils, the MCC model can predict certain strain-softening behaviour (Britto and Gunn, 1987) for stress paths that approach the CSL from above (i.e., from stress ratios (q/p') exceeding the critical state value, M). However, for most natural clayey deposits, the degree of softening is often much more than is predicted by the MCC model. Furthermore, strain-softening is also observed for normally consolidated clayey soils, and the conventional MCC model is unable to capture this type of softening. Using the advantages of the relative simplicity of the MCC model, the following method is proposed to simulate the enforced strain-softening behaviour during undrained and/or partially drained loading.

Enforced Strain-Softening

The conditions for enforcing strain-softening are: (a) the stress state remains on a current yield surface and on the CSL in p' - q space, and (b) the shear strain increases and is larger than the past maximum shear strain a soil element has experienced. As shown in Fig. 2, if the incremental shear strain $\Delta\varepsilon_s > 0$ (path 1 in Fig. 2), then strain-softening will occur. If $\Delta\varepsilon_s \le 0$ (paths 2, 3 and 4 in Fig. 2), there will be no enforced strain-softening and the stress-strain relationship of a soil element will be fully controlled by the conventional MCC model.

Strain Increments

Assumption 1: It is assumed that during the softening process the strain increments can still be calculated by the MCC model, i.e., there is no overall volumetric strain increment ($\Delta\varepsilon_v = 0$) and the shear strain increment ($\Delta\varepsilon_s$) is indefinite. For a real boundary value problem, the shear strain will be limited by (external) kinematic constraints.

Stress Increments

Assumption 2: During softening, an empirical relationship between incremental total shear strain ($\Delta\varepsilon_s$) and incremental deviator stress (Δq) is assumed, as shown in Fig. 3. When the stress state is on a current yield surface and on the projected CSL, all of the incremental shear strain will be plastic (Δq = 0). This empirical relation is expressed as

$$\Delta q = \alpha \cdot \Delta\varepsilon_s \tag{1}$$

where α is the slope of the strain-softening path, referred to as the softening rate. In Fig. 3, ε_{scs} and q_{cs} are the shear strain and deviator stress when the stress state first reaches the CSL in p' - q space and is also on a current yield surface. These values are determined by the MCC model and not pre-defined. Since for general loading cases q_{cs} is not known, the value of Δq can not be properly specified *a priori*. Therefore, it is more convenient to use a ratio (SR) between the residual deviator stress q_{re} and q_{cs} as follows:

$$SR = \frac{q_{re}}{q_{cs}} \tag{2}$$

so that $\Delta q = (1 - SR) \cdot q_{cs}$. $\Delta\varepsilon_s$ and SR will be used as the two additional model parameters defining the strain-softening. Following Carter and Liu (2005), it is assumed that during strain-softening, the effective stress path is only allowed to move along on the CSL in a p'-q plot and the effective mean stress increment $\Delta p'$ can be therefore determined as follows.

$$\Delta p' = \Delta q / M \tag{3}$$

where M is the slope of the CSL in a p'-q plot. Let us denote the stress state in terms of the values of q and p' at the beginning and the end of a load increment, i.e., as (q_b, p'_b) and (q_e, p'_e), respectively, then $q_e = q_b + \Delta q$ and $p'_e = p'_b + \Delta p'$. However, for two dimensional (2D) problems the complete state of stress is necessarily described by four (4) quantities, while for three dimensional (3D) problems six (6) are required. Knowing only q_e and p'_e, i.e., only two stress quantities, we can not determine the general stress state at the end of a load increment.

Assumption 3: To overcome this difficulty it is assumed that during softening all stresses reduce by the same proportion with respect to their values at the beginning of a load increment. For a 2D problem, this assumption can be expressed as follows:

$$\frac{\sigma'_{xe}}{\sigma'_{xb}} = \frac{\sigma'_{ye}}{\sigma'_{yb}} = \frac{\sigma'_{ze}}{\sigma'_{zb}} = \frac{\tau_{xye}}{\tau_{xyb}} = \frac{q_e}{q_b} \tag{4}$$

where σ'_x, σ'_y, σ'_z are normal effective stresses in the x, y and z directions, respectively, and τ_{xy} is the shear stress in the x-y plane. Equation (4) represents 4 linear equations from which the stress state at the end of a load increment can be obtained in terms of general stress variables. Obviously, for a drained triaxial test, linear reduction of stresses is not applicable when the effective confining stress does not change. For undrained and/or partially drained triaxial tests, linear reduction of stresses is possible. In these cases reduction of confining effective stress implies an increase in excess pore pressure. Therefore, the proposed method is limited to undrained and/or partially drained loading conditions.

Stress Equilibrium

With the method described above, the stress state at the end of a load increment is enforced or somewhat "artificially" determined. Therefore, force equilibrium is not guaranteed. To maintain the equilibrium of a computed stress field, iteration is required.

It is worth mentioning that the approach proposed here is not completely rigorous in the applied mechanics sense. Rather, it is a pragmatic approach designed to obtain approximate engineering solutions to geotechnical problems involving strain-softening, particularly of soft clayey soils.

Table 1 Adopted model parameters

Case	λ	κ	e_{cs}	M	μ	$\Delta\varepsilon_{sL}$	SR	σ'_{h0} (kPa)	σ'_{v0} (kPa)	p'_{y0} (kPa)
Verify the model	0.3	0.03	2.25	1.2	0.3	0.03, 0.05	0.4, 0.6	50	50	50, 100, 150
Ariake clay	0.55	0.05	4.87	1.6	0.3	0.07	0.7	23	46	57
Lime stabilized	0.90	0.03	8.8	2.0	0.3	0.05	0.7	127, 382, 510	127, 382, 510	1064

Note: λ and κ are slopes of virgin loading, unloading-reloading lines in an e - lnp' plot (e is void ratio) respectively; e_{cs} is void ratio at CSL with a mean effective stress p' = 1 kPa; M is slope of CSL in q-p' plot; μ is Poisson's ratio; σ'_{h0} *and* σ'_{v0} are initial horizontal and vertical effective stresses respectively; p'_y is the initial size of yield locus.

PERFORMANCE OF THE PROPOSED METHOD

The proposed method has been incorporated into the CRISP-AIT program (Chai, 1992), which is based on the original CRISP program (Britto and Gunn, 1987), to simulate strain-softening behaviour. To check the performance of the method, single element analyses were conducted under undrained triaxial compression conditions.

The element used in these single element studies was an 8-node quadrilateral deforming under axisymmetric conditions with full integration (3×3 integration points). The stress state of the central integration point is used in the following presentation. The element size and boundary conditions are shown in Fig. 4. The model parameters adopted are listed in Table 1. Two softening rates (relatively high and relatively low) and three initial stress states (normally and overconsolidated) were considered. Shear strain (ε_s) versus deviator stress (q) and excess pore pressure (u) curves and effective stress paths in p'-q space are plotted and discussed.

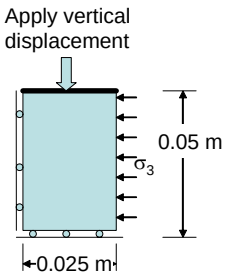

Fig. 4 Element size and boundary conditions

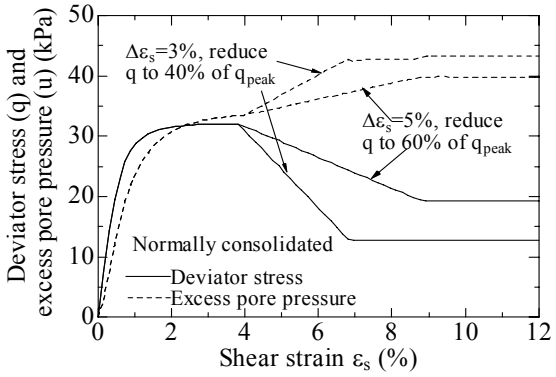

Fig. 5 ε_s-q and ε_s -u curves (NC)

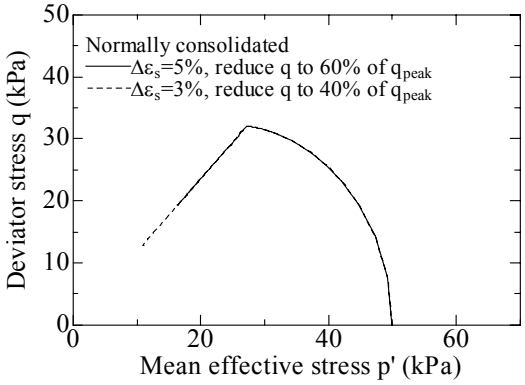

Fig. 6 p'-q plots (NC)

Normally Consolidated (NC) State

Simulated ε_s-q and ε_s -u curves and p'-q plots are given in Figs 5 and 6, respectively. It can be seen that the analysis yielded both ε_s-q curves and p'-q plots as desired. During the softening process u increased. This is because under a constant total confining stress, reducing effective horizontal stress results in an increase in excess pore pressure in order to maintain equilibrium.

Figures 5 and 6 represent the strain-stress state at the centre of the element (9th integration point). It has been observed that during the softening process the stress state within the element is uniform up to a certain stage and then the stress state becomes non-uniform, presumably due to round-off errors. This must be a numerical artifice, since theoretically the behaviour of the single element should be homogeneous. The total shear strain at which the stress states at the integration points within the element start to show slight differences (of about 0.001 kPa) is defined here as the threshold shear strain, ε_{s1}. The values of ε_{s1} are listed in Table 2. For the NC state, the value of ε_{s1} is about 7.1% for the lower softening rate case ($\Delta\varepsilon_s$ = 5%, SR = 0.6) and about 5.9% for the higher softening rate case ($\Delta\varepsilon_s$ = 3%, SR = 0.4). The higher the softening rate, the lower is the value of ε_{s1}. After the threshold shear strain, the differences in stress state at the individual integration points gradually increased and shear strain localization occurred within the element. At certain integration points, unloading actually occurred. The location of the strain localization appears to be random, but as this appears to be a numerical artifice, it is probably dependent on the particular shape of the element used in the modelling, the size of the incremental displacements, the allowable maximum unbalanced load during the iteration, and the stress path, as well as being computer dependent. The values listed in Table 2 were obtained using double-precision arithmetic with a FORTRAN program compiled by the f77 compiler, running on a UNIX workstation (Solaris-10). The adopted maximum allowable unbalanced load was 3% of the nodal force. It is noted that strain-softening is an unstable process and any kinematically allowable displacement can occur. In a boundary value problem, the softening zone will be surrounded by elements which are not softening and the shear strains in the softening region are then restricted by the surrounding material and/or the boundary conditions. Therefore, the random shear strain localization phenomenon which appeared during the strain-softening

Table 2 Threshold shear strains

No.	p'_0 (kPa)	p'_y (kPa)	Shear strain, ε_{s1} (%)	
			Lower softening rate $\Delta\varepsilon_s$=5%, SR=0.6	Higher softening rate $\Delta\varepsilon_s$=3%, SR=0.4
1 (NC)	50	50	7.1	5.9
2 (OC-1)	50	100	4.8	3.2
3 (OC-2)	50	150	7.8	6.7

in the single element analyses may not be a significant issue in more general boundary value problems.

Over-Consolidated State-1 (OC-1)

For this case $p'_0 = p'_{cs0}$, where p'_0 is the initial effective mean stress and p'_{cs0} is the initial mean stress on the CSL and on the initial yield surface. As for the NC case, the ε_s-q and ε_s-u curves and the p'-q plots for the OC-1 case are as given in Figs 7 and 8, respectively. The values of ε_{s1} are also given in Table 2. For this case, there is a small jump on the simulated ε_s-u curves after the threshold shear strain (ε_{s1}) has been mobilized, but again this is considered to be a numerical problem rather than a physical phenomenon. Since the value of p'_0 was selected to be equal to p'_{cs0}, when the stress state reached the initial yield surface, the softening commenced, and the values of ε_{s1} are relatively small (Table 2).

Over-Consolidated State-2 (OC-2)

For this case $p'_0 < p'_{cs0}$ and the strain-softening process of a heavily overconsolidated soil is simulated. From Figs 9 and 10 it can be seen that although there are small numerical oscillations for the higher softening rate case, generally the analyses simulated the ε_s-q, ε_s-u and

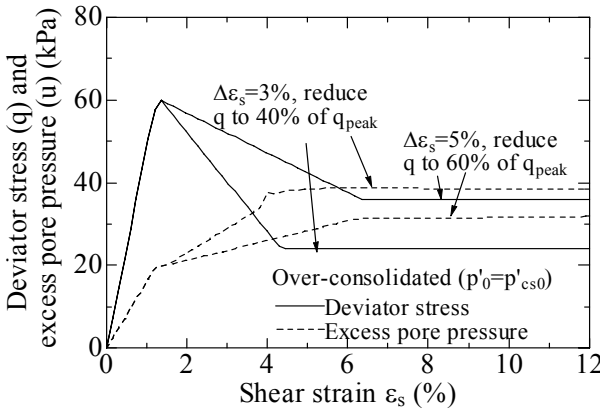

Fig. 7 ε_s-q and ε_s-u curves (OC-1)

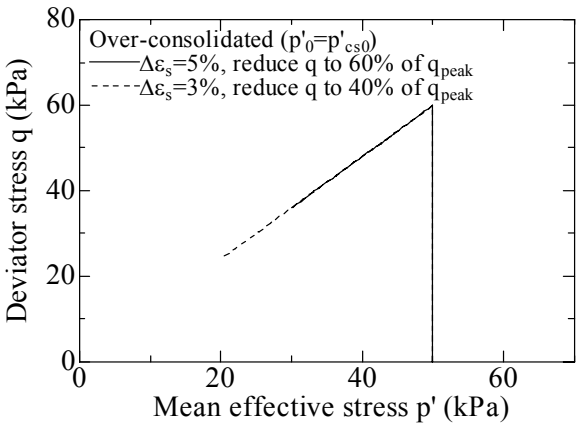

Fig. 8 p'-q plots (OC-1)

p'-q relationships well. Under the constant confining stress condition, after the stress state reached the initial yielding surface above the CSL and moved toward CSL, p' increased and u reduced (Fig. 9). When softening started there was an increase in u, as occurred for the NC and OC-1 cases. In this case, the stress path approached the CSL from above the CSL and the values of the threshold shear strain ε_{s1} were relatively large (Table 2).

The results presented in Figs 5 to 10 demonstrate that generally the proposed method simulated well the strain-softening process of a single element of soil.

SIMULATING STRAIN-SOFTENING OF NATURAL ARIAKE CLAY

Ariake clay is widely deposited around the Ariake Sea in Kyushu, Japan with a thickness of 10 to 30 m. Ariake clay is dominated by smectic clay minerals (Ohtsubo et al., 1995) and has a natural water content of more than 100%. The clay is highly compressible and micro-structured. Tanaka (2000) reported triaxial undrained compression test results using undisturbed Ariake clay samples. The samples were obtained from Hizen-Kashima, Saga, Japan. The soil profile at the site is shown in Fig. 11 (after Tanaka, 2000). Tanaka used this site to check the qualities of 6 different samplers. Triaxial compression tests were conducted using undisturbed samples and the stress-strain conducted by firstly reconsolidating the samples under their corresponding in-situ stresses and then sheared under undrained condition. Since the test results for the samples at 10 m depth were reported in detail, they have also been simulated by the proposed method and compared with the test data. Only the test data for samples obtained using the Japanese thin-wall sampler (JPN), and a block sampler developed by Sherbrooke University, Canada (Sherbrooke) are considered here.

The same as for verifying the proposed model, one 8-node quadrilateral element was used to simulate the triaxial compression test under axisymmetric conditions. The model parameters adopted are listed in Table 1.

The consolidation test results for the samples at 11 m depth (no data reported for 10 m depth) are as shown in Fig. 12 (data points from Tanaka, 2000). Based on the results in Fig. 12, the values of λ, κ and e_{cs} were evaluated and listed in Table 1. The values for μ and M were assumed empirically. The in-situ effective stresses (σ'_{ho}, σ'_{vo}) were evaluated by using the natural water content given in Fig. 11 and assuming that the groundwater level was 1.0 m below the ground surface and the density of soil particles is 26.5 kN/m^3. Referring to Fig. 12, an initial size of the yield locus of 57 kPa (adopting a maximum vertical consolidation stress

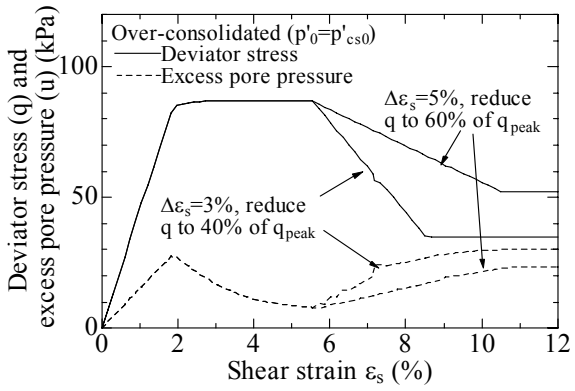

Fig. 9 ε_s-q and ε_s-u curves (OC-2)

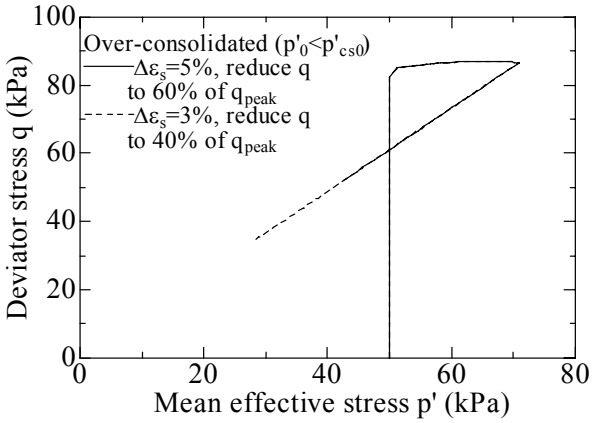

Fig. 10 p'-q plots (OC-2)

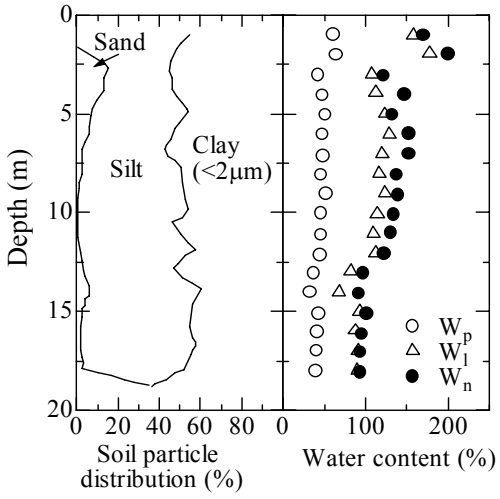

Fig. 11 Soil profile at Hizen-Kashima, Saga, Japan

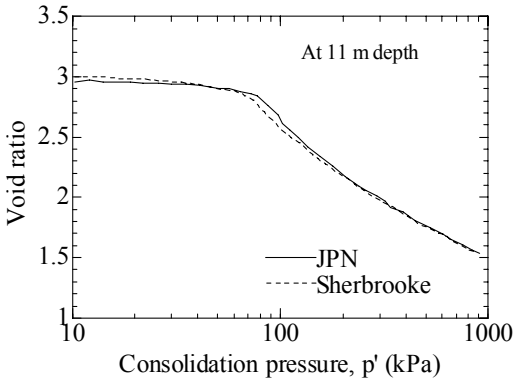

Fig. 12. Consolidation curves for the samples at 11 m depth (data points from Tanaka, 2000).

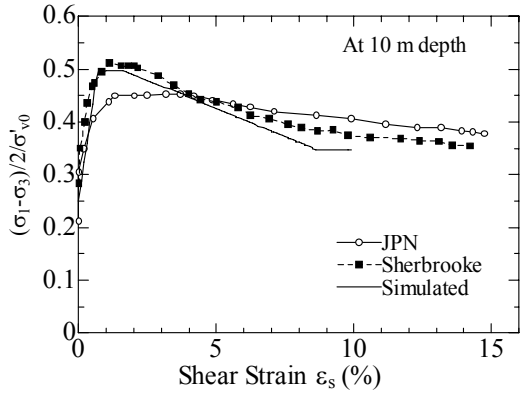

Fig. 13. Comparison of shear strain versus normalized deviator stress curves of undisturbed Ariake clay

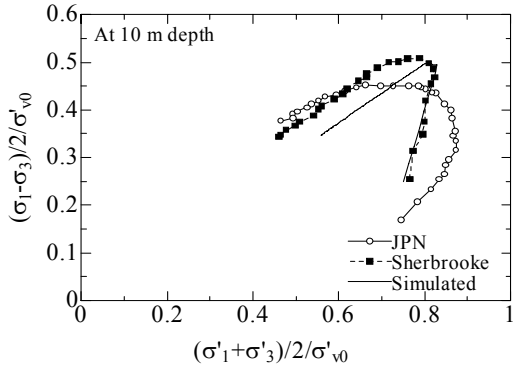

Fig. 14. Comparison of effective stress path of undisturbed Ariake clay

σ'_{vm} = 70 kPa and an at rest earth pressure coefficient k_0 value of 0.5) was estimated. The strain-softening parameters $\Delta\varepsilon_{sL}$ and SR were determined by back fitting simulated results with the test data.

Comparison of simulated shear strain (ε_s) versus normalized deviator stress ((σ_1-σ_3)/(2σ'_{v0})) is shown in Fig. 13, where σ_1 and σ_3 are maximum and minimum normal stresses and σ'_{v0} is the initial vertical effective stress. The simulated results compare well with the results of the sample obtained by the Sherbrooke sampler. Among the samplers investigated by Tanaka (2000), the Sherbrooke sampler was deemed as providing the highest quality. The sample obtained is cylindrical with a diameter of 350 mm and height of 250 mm. The normalized effective stress paths are compared in Fig. 14

using the variables adopted by Tanaka (2000). The simulation yielded a close match to the results using the sample obtained by the Sherbrooke sampler up to the CSL. It seems that the slope of the CSL (M value) is larger than the value of 1.6 used (corresponding to an internal friction angle of about 39°). After the peak strength, the simulated CSL is parallel to the line formed by the test data (Sherbrooke sampler). The simulated CSL will pass through the origin if extended, but if the line formed by the test data is extended, it will not pass the origin. It could be argued that the undisturbed Ariake clay sample may possess true or at least apparent cohesion, which the MCC model cannot consider. For the test data obtained from the samples retrieved using the JPN sampler, even the initial stress state is different from that of the samples recovered from the Sherbrooke sampler (lower initial deviator stress). Although there is no explanation about this difference in the original paper (Tanaka, 2000), the samples may have been obtained at slightly different depths and/or locations.

The excess pore water pressure (u) was not reported by Tanaka (2000). However, by personal communication the test data have been kindly provided by Prof. H. Tanaka of Hokkaido University, Japan. The u versus ε_s curves are compared in Fig. 15. Both test data and simulated results indicate that u increased during the soften process. This is because reduction of effective mean stress requires an increase in u to maintain equilibrium of the system. However, the simulated values are lower than the test data. As can be seen from Fig. 14 the simulated effective stress path during softening is on the right hand side of the test data, which means that for a given deviator stress, the simulated mean effective stress is larger than the test value and thus the excess pore pressure is less than the test value. This suggests that the results in Figs 14 and 15 are consistent. It is considered that the small jump in the simulated curve shown at about 6% shear strain is probably due to numerical error.

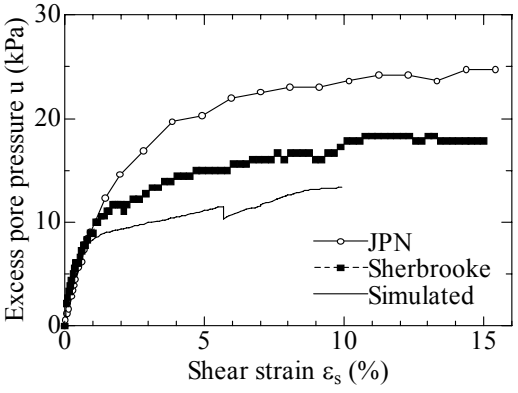

Fig. 15 Comparison of excess pore pressure variation

SIMULATING STRAIN-SOFTENING OF LIME-STABILIZED ARIAKE CLAY

Since Ariake clay is a very soft soil deposit, most engineering activities in this region usually involve some type of ground improvement. Stabilizing the Ariake clay by mixing cement or lime into the ground is a commonly used method. Cement or lime stabilized soils normally exhibit strain-softening behaviour. Yamadera (1999) reported some triaxial test results of lime-stabilized Ariake clay samples, which will be considered here.

The Ariake clay tested was sampled from the Ashikari District, in Saga, Japan, with natural water content, W_n, of 136 – 159%, natural void ratio, e, of 3.6 – 4.2, liquid limit, W_l, of 112%, and plastic limit, W_p, of 70%. Quick lime, of 10% by dry weight, was mixed into the soil (10% lime sample) to improve its mechanical properties. The e – ln(p') relationships of the remoulded and the lime-stabilized samples (cured for 28 days) are shown in Fig. 16. From the curve of the 10% lime sample, a value λ of 0.9, κ of 0.03, and initial voids ratio of 3.25 were evaluated. The size of the yield locus of 1064 kPa was estimated using yield values of the vertical and horizontal effective stresses of 1400 kPa and 700 kPa, respectively. The adopted initial isotropic consolidation stresses (p'_o) were 127, 382 and 510 kPa. For this lime-stabilized soil, a value of M of 2.0 (corresponding to an internal friction angle of about 49°) was assumed. This is a relatively high value of the friction parameter but it is consistent with the experimental data for this lime-treated clay over the range of stresses being considered here. The test data show that in the p' – q plot, when the confining stress is more than about 3000 kPa, the slope of CSL became smaller and line was curved (Yamadera 1999). The softening parameters and Poisson's ratio were assumed, as shown in Table 1.

Simulated ε_s – q curves are compared with test data in Fig. 17. For the p'_o = 382 and 510 kPa cases, the simulation is fair, but for the p'_o = 127 kPa case,

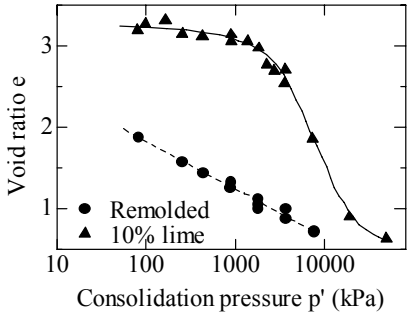

Fig. 16 e - ln(p') curves of remoulded and lime stabilized samples

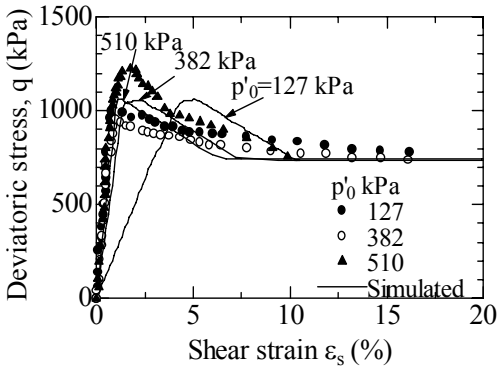

Fig. 17 Comparison of $\varepsilon_s - q$ curves of lime stabilized Ariake clay

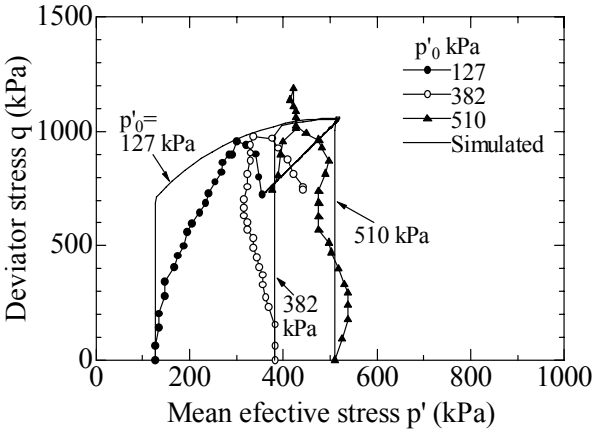

Fig. 18 Comparison of effective stress paths of lime stabilized Ariake clay

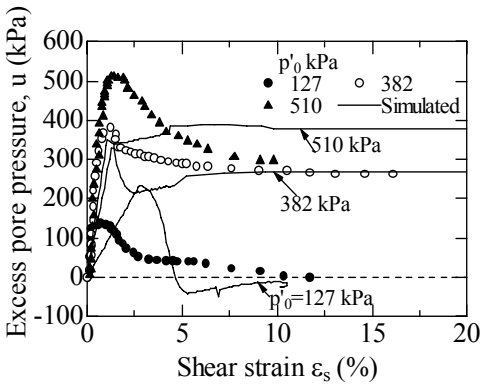

Fig. 19 Comparison of $\varepsilon_s - u$ curves of lime stabilized Ariake clay

the simulation significantly under-estimated the initial stiffness of the soil. For all three cases, initially the samples were in the elastic range, and for the MCC model the soil stiffness is proportionally related to its effective mean stress and inversely related to the κ value (= 0.03 in this case). The predicted stiffness for the p'_0 = 127 kPa case was lower than the observed stiffness. It is suggested that values of the initial stiffness of most cement and/or lime-stabilized soils are not linearly related to their confining stress and higher values need to be considered when simulating the mechanical behaviour of this kind of soil. Another discrepancy between the test data and the simulated results concerns the values of peak strength. Test data show that the peak strength at p'_o = 510 kPa is obviously higher than that for the case of p'_o = 127 kPa, but the simulated results do not show an obvious difference. For all three cases, the effective stress path approached the CSL from above (Fig. 18). When a stress path approaches the CSL from above, the MCC model will simulate shrinkage of the yield locus to compensate for the elastic volumetric strain induced by increasing p'. In cases where $p' < p'_y/2$ (p'_y is the size of current yield locus), the closer the value of p' to $p'_y/2$, the less the shrinkage of the yield surface (reduction in p'_y) and the larger the peak strength. Since the difference between the adopted λ and κ values is large, the compressive elastic volumetric strain induced by increasing p' is relatively small, and consequently the reduction in p'_y is small. As a result, there is not much difference in the simulated peak strength. Although the exact reason for this discrepancy is not clear, it probably due to non-uniformity of the samples tested, and/or the limitation of using MCC model to simulate the behaviour of the lime-stabilized Ariake clay.

Figure 18 compares the effective stress paths. Although there are discrepancies, generally the simulation gives a fair match to the test data. One aspect of the observed response requires further explanation. The data points were read from a figure given by Yamadera (1999) with a range of x and y axes of 10,000 kPa. For the three lines considered here, the points close to the CSL were mixed together and cannot be clearly identified. The points plotted in Fig. 18 for those locations are "best estimations".

Comparison of excess pore water pressure is given in Fig. 19. The simulation yields a fair prediction of the test data, but there are several discrepancies. Firstly, for the p' = 127 kPa case, the predicted maximum u value and the shear strain corresponding to the maximum value are larger than the test data. This is consistent with the results shown in Fig. 17 and is believed to be caused by under-estimation of the initial stiffness of the sample. Secondly, the predicted maximum value for the p' = 510 kPa case is smaller than the test data and the form of variation is also different. The test data showed an obvious reduction after the peak value, but the simulation did not predict this, because the initial effective mean stress is very close to $p'_{yo}/2$ (i.e., before softening, there is not much increase in p' and therefore little reduction in u). Generally, the simulation predicts a reduction of u value when the stress path moves

towards the CSL from above it and an increase during the softening process.

CONCLUSIONS

A method for modelling the strain-softening behaviour of clayey soil under undrained and/or partially drained conditions is proposed. The method is based on the Modified Cam clay (MCC) soil model. It is assumed that during a softening process, the strain increments can still be calculated by the MCC model, but the effective stress path is forced to follow the projection of the critical state line (CSL) in a p' - q plot (i.e., $q = M\,p'$). Therefore, the method is not rigorous in the applied mechanics sense, rather it is a pragmatic approach.

The proposed method has been incorporated into a finite element code CRISP-AIT, which is based on the original CRISP program. Single element analyses of clays deforming under undrained triaxial conditions were conducted to verify the performance of the proposed method. The proposed method has been applied to simulate the mechanical behaviour of undisturbed Ariake clay and lime-stabilized Ariake clay samples tested under undrained conditions. Comparing the simulated results with the test data indicates that the method simulated both the shear strain versus deviator stress and the effective stress paths of the undisturbed Ariake clay samples and the lime stabilized Ariake clay samples reasonably well. However, the result also showed that in case of the lime-stabilized Ariake clay, the adoption of a high initial stiffness under lower confining stress should be considered. It is suggested that the method adopted in this study can be used to analyze geotechnical problems involving strain-softening behaviour of soft clayey soils under undrained condition with reasonable accuracy.

ACKNOWLEDGEMENT

This study is part of a special research program partially financially supported by the Institute of Lowland Technology, Saga University, Japan. Partial support from the Australian Research Council is also gratefully acknowledged. Prof. H. Tanaka at Hokkaido University, Japan, provided test data on excess pore pressure of natural Ariake clay samples. His generosity is greatly appreciated. Sincere thanks are extended to Dr. H. Poorooshasb, President of International Association of Lowland Technology, for his valuable comments during the preparation of this paper.

REFERENCES

Adachi T., Oka F., Hirata T., Hashimoto T., Nagaya J., Mimura M. and Pradhan T. B. S. (1995). Stress-strain behavior and yielding characteristics of Eastern Osaka clay, Soils and Foundations, 35(3): 1-13.

Britto A. M. and Gunn M. J. (1987). Critical state soil mechnics via finite elements, Ellis Horwood Limited, p. 486.

Carter J. P. and Liu M. D. (2005). Review of the structured Cam clay model, Soil Constitutive Models: Evaluation, Selection and Calibration, ASCE, Geotechnical Special Publication No. 128: 99-132.

Chai J.-C. (1992). Interaction between grid reinforcement and cohesive-frictional soil and performance of reinforced wall/embankment on soft ground, PhD Dissertation, Asian Institute of Technology, Bangkok, Thailand.

Ohtsubo K., Egashira K. and Kashima K. (1995). Depositional and post-depositional geochemistry, and its correlation with the geotechnical properties of marine clays in Ariake Bay, Japan. Geotechnique, 45(3): 509-523.

Potts D. M., Dounias G. T. and Vaughan P. R. (1990). Finite element analysis of progressive failure of Carsington embankment, Géotechnique 40(1): 79-101.

Roscoe K. H. and Burland J. B. (1968). On the generalized stress-strain behavior of 'wet' clay, Engineering Plasticity (edited by J. Heyman and F.A. Leckie), Cambridge University Press: 535-609.

Tanaka H. (2000). Sample quality of cohesive soils: lessons from three sites, Ariake, Bothkennar and Drammmen. Oils and Foundations, 40(4): 57-74.

Tanaka H., Shwakoti D. R., Mishima O., Watabe Y. and Tanaka M. (2001). Comparison of mechanical behavior of two overconsolidated clays: Yamashita and Louiseville clays, Soils and Foundations, 41(4): 73-87.

Yamadera A. (1999). Microstructural study of geotechnical characteristics of marine clays. PhD Dissertation, Saga University, Saga, Japan.